

Insertion Profiles of 4 Headless Compression Screws

Adam Hart, MD, Edward J. Harvey, MD, Louis-Philippe Lefebvre, MSc, Francois Barthelat, PhD, Reza Rabiei, PhD, Paul A. Martineau, MD

Purpose In practice, the surgeon must rely on screw position (insertion depth) and tactile feedback from the screwdriver (insertion torque) to gauge compression. In this study, we identified the relationship between interfragmentary compression and these 2 factors.

Methods The Acutrak Standard, Acutrak Mini, Synthes 3.0, and Herbert-Whipple implants were tested using a polyurethane foam scaphoid model. A specialized testing jig simultaneously measured compression force, insertion torque, and insertion depth at half-screw-turn intervals until failure occurred.

Results The peak compression occurs at an insertion depth of -3.1 mm, -2.8 mm, 0.9 mm, and 1.5 mm for the Acutrak Mini, Acutrak Standard, Herbert-Whipple, and Synthes screws respectively (insertion depth is positive when the screw is proud above the bone and negative when buried). The compression and insertion torque at a depth of -2 mm were found to be 113 ± 18 N and 0.348 ± 0.052 Nm for the Acutrak Standard, 104 ± 15 N and 0.175 ± 0.008 Nm for the Acutrak Mini, 78 ± 9 N and 0.245 ± 0.006 Nm for the Herbert-Whipple, and 67 ± 2 N, 0.233 ± 0.010 Nm for the Synthes headless compression screws.

Conclusions All 4 screws generated a sizable amount of compression (> 60 N) over a wide range of insertion depths. The compression at the commonly recommended insertion depth of -2 mm was not significantly different between screws; thus, implant selection should not be based on compression profile alone. Conically shaped screws (Acutrak) generated their peak compression when they were fully buried in the foam whereas the shanked screws (Synthes and Herbert-Whipple) reached peak compression before they were fully inserted. Because insertion torque correlated poorly with compression, surgeons should avoid using tactile judgment of torque as a proxy for compression.

Clinical relevance Knowledge of the insertion profile may improve our understanding of the implants, provide a better basis for comparing screws, and enable the surgeon to optimize compression. (*J Hand Surg* 2013;38A:1728–1734. Copyright © 2013 by the American Society for Surgery of the Hand. All rights reserved.)

Key words Headless compression screw, insertion depth, insertion torque, interfragmentary compression, scaphoid fracture.

THE SCAPHOID IS the most commonly fractured carpal bone, accounting for approximately 60% of all carpal fractures¹ and an estimated incidence of 30 fractures per 100,000 person-years.² This

injury occurs predominantly in young healthy adults³ and is associated with a high incidence of delayed union, nonunion, and osteonecrosis owing to the tenuous blood supply to the bone.^{4,5} Management of these

From the Division of Orthopedic Surgery, McGill University Health Centre; the Department of Mechanical Engineering, McGill University, Montreal; and the National Research Council Canada, Boucherville, Quebec, Canada.

Received for publication February 2, 2013; accepted in revised form April 23, 2013.

This study was made possible by a research grant from the Canadian Institute of Health Research.

No benefits in any form have been received or will be received related directly or indirectly to the subject of this article.

Corresponding author: Adam Hart, MD, Division of Orthopedic Surgery, McGill University Health Centre, 1650 Cedar Avenue, A5-175.1, Montreal, Quebec, Canada H3G 1A4; e-mail: adam.hart@mail.mcgill.ca.

0363-5023/13/38A09-0010\$36.00/0
<http://dx.doi.org/10.1016/j.jhssa.2013.04.027>

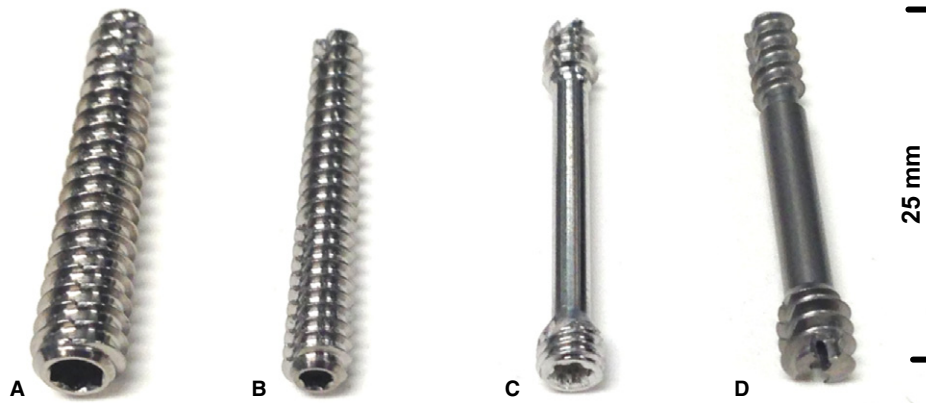


FIGURE 1: Four HCSs tested. **A** Acutrak Standard. **B** Acutrak Mini. **C** Synthes 3.0. **D** Herbert-Whipple.

injuries was transformed in the 1980s with the introduction of the scaphoid specific Herbert screw⁶ and subsequent screw variations. A headless screw generates interfragmentary compression through differential pitches between the leading and the trailing threads. The compression thereby provides rigid internal fixation without the intra-articular prominence of standard headed screws. A headless compression screw (HCS) has become the implant of choice for the internal fixation of displaced and nondisplaced scaphoid fractures.^{7,8}

Given the popularity of the HCS, sundry commercial designs have emerged, each with its own variation in thread pitch, shaft diameter, and shape. Despite an abundance of recent papers describing biomechanical testing of these screws in both human cadaver^{9–15} and polyurethane foam^{16–22} scaphoid models, the results are discordant, and there is little consensus on optimal screw design. Moreover, the vast majority of studies report peak compression force; however, it is unlikely this force is achieved consistently in clinical practice. In the absence of a load cell measuring compression, the surgeon must rely on screw position (insertion depth) and tactile feedback from the screwdriver (insertion torque), which may or may not correlate with compression. Rather than using peak compression as the end point to compare screws, the compression in relation to insertion depth and torque (the insertion profile) is of greater clinical interest. Knowledge of such a profile would improve our understanding of the implant, provide a better basis for comparing HCSs, and enable the surgeon to optimize compression.

The purpose of this study was to determine the insertion profiles of 4 popular, commercially available HCSs. Using a customized setup, both interfragmentary compression and insertion torque were measured simultaneously as the test screws

were driven into a polyurethane foam scaphoid bone model. The goals of our study were to identify the relationship between the compression force, the insertion torque, and the insertion depth; to determine the insertion depth that yields peak compression for each screw; and to measure compression and torque at an insertion depth of -2 mm below the cortex. This depth maximizes screw length while ensuring a buried depth of -2 mm below the articular cartilage and is frequently recommended in the literature.⁸

MATERIALS AND METHODS

Implants

Four commercially available HCSs were tested (Fig. 1). All screws were chosen to have similar length (24–25 mm) in order to control for bone purchase. The Acutrak Standard (Acumed, Hillsboro, OR) is a highly polished titanium, conically shaped, self-tapping, fully threaded, cannulated screw with a variable thread pitch spanning the entire screw. It has a distal outer diameter (DOD) of 3.3 mm, and proximal outer diameter (POD) of 4.4 mm. The Acutrak Mini (Acumed, Hillsboro, OR) is a scaled-down version of the Acutrak Standard with DOD and POD of 2.8 mm and 3.5 mm, respectively. The Synthes 3.0-mm HCS (DePuy Synthes, West Chester, PA) is a cannulated 316L stainless steel, self-drilling, and self-tapping headless screw with DOD and POD of 3.0 mm and 3.5 mm, respectively. A smooth shank that allows for precompression to be applied during screw insertion separates the distal and proximal threads. The Herbert-Whipple HCS (Zimmer, Warsaw, IN) is a modified version of the original Herbert screw with a slightly larger diameter to accommodate cannulation and has self-tapping leading threads. Made of titanium (Ti-6Al-4V alloy), the DOD and POD are 3 mm and 3.85

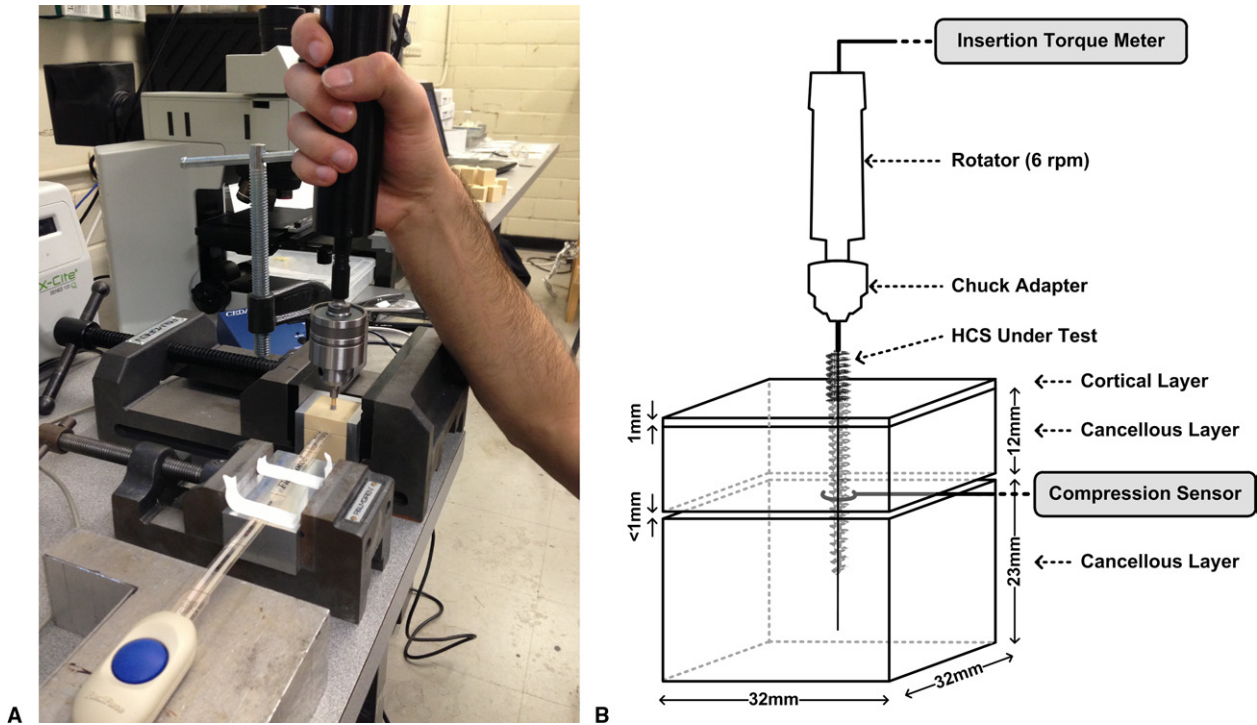


FIGURE 2: Test setup. **A** Photograph. **B** Schematic.

mm, respectively, separated by a smooth 2.5-mm-diameter shank between proximal and distal threads. The Acutrak screws generate compression through the combination of a conically shaped shaft and variable thread pitch along the screw whereas the shanked screws create compression with 2 constant but different thread pitches at either end of the screw.

Scaphoid bone model

In order to mitigate testing variability between samples, a rigid polyurethane foam model (1522-03, Pacific Research Laboratories, Vashon, WA) was used to simulate the scaphoid fracture. The biomechanical properties of the foam are well controlled²³ and were selected to best approximate scaphoid cancellous bone of a young adult^{24,25}—comprising a density of 0.32 g/mL and compressive, tensile, and shear moduli of 210 MPa, 284 MPa, and 49 MPa, respectively. The foam was machined by computer numerical control into 32 mm × 32 mm × 35 mm blocks, and a diamond saw was used to create a linear osteotomy 12 mm from the surface. A 1-mm layer of denser foam (0.64 g/mL) was laminated to the surface to represent cortical bone.

Testing procedure

The test setup is shown in Figure 2. A custom testing jig was used to hold the polyurethane foam blocks and prevent rotation during screw insertion. The blocks

were free to slide vertically within the clamps as compression was applied. In order to minimize the displacement of the simulated fractures, an ultrathin load sensor was employed. The FlexiForce (A201, Tekscan, Boston, MA) is a 0.13-mm-thick piezoresistive force sensor printed onto a flexible circuit board. A 5-mm hole between 2 thin metal washers was placed at the center of the sensing head in order to accommodate a screw. The load sensor was then sandwiched between 2 foam blocks, and the HCS under test was placed through the center of the sensor (Fig. 2B). The total displacement created by the load sensing apparatus was less than 1 mm.

The HCSs were inserted according to their respective manufacturer's guidelines into an intact, new foam block. A precompression force of 70 to 80 N was applied to the Synthes screws using the manufacturer's specific compression sleeve and screwdriver. A torque meter (Imada, Northbrook, IL) was used to advance the screws in half-turn intervals while recording the insertion torque, insertion depth, and interfracture compression. A time delay of 10 seconds between intervals was used to ensure stable measurements. Insertion depth was measured by digital caliper to the nearest 0.1 mm and defined as the distance from the proximal tip of the screw to the surface of the foam (positive when the

screw was proud and negative when the screw was buried in the foam). Each test was stopped after a sustained drop in compression was observed (representing loss of fixation). The experiment was repeated 5 times for each HCS type for a total of 20 tests.

Statistical methods

Compression and insertion torque profiles were generated for each trial by synchronizing the data and plotting them versus screw insertion depth. Composite plots taking the mean of the 5 trials were also generated with error bars representing the standard error of the mean. Descriptive statistics and 1-way analysis of variance were used to analyze the compression and torque values.

Preliminary validation of the experimental setup yielded compression measurements with a standard deviation of approximately 20 to 25 N. In order to have a standard error of less than 10% (10 N assuming compression forces of approximately 100 N), a sample size of 5 was needed.

RESULTS

Interfragmentary compression and insertion torque profiles were obtained for each screw type as illustrated in Figure 3 for the Herbert-Whipple implant. The 5 tests for each screw were then combined to produce the composite profiles shown in Figure 4 where the error bars represent the standard error of the mean. The peak compression occurred at an insertion depth of -3.1 mm, -2.8 mm, 0.9 mm, and 1.5 mm for the Acutrak Mini, Acutrak Standard, Herbert-Whipple, and Synthes screws, respectively.

The compression and insertion torque at a depth of -2 mm below the surface (recommended insertion depth⁸), from greatest to least compression, were found to be from the Acutrak Standard (113 ± 18 N, 0.348 ± 0.052 Nm), Acutrak Mini (104 ± 15 N, 0.175 ± 0.008 Nm), Herbert-Whipple (78 ± 9 N, 0.245 ± 0.006 Nm), and Synthes (67 ± 2 N, 0.233 ± 0.010 Nm) HCSs. Analysis of variance demonstrated no significant difference in compression or torque between any of the screws ($P > .05$).

DISCUSSION

Bone quality, fracture geometry, and patient comorbidities are uncontrollable factors affecting healing; however, the choice of implant may be at the surgeon's discretion. For this reason, there has been a flurry of studies evaluating the biomechanical advantage of 1 HCS over the other. Investigations have looked at decay in peak compression over time,¹³ compression

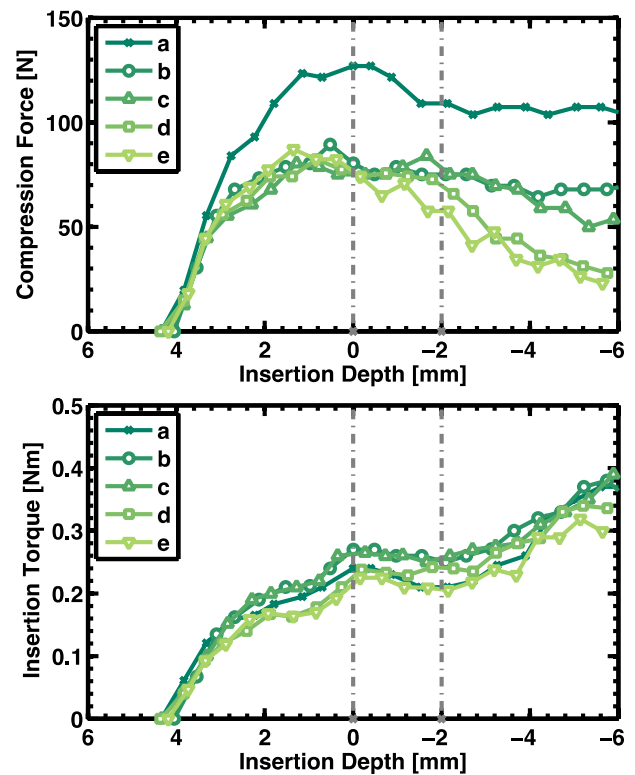


FIGURE 3: Individual tests (a–e) of the Herbert-Whipple screw: interfragmentary compression profile (top) and insertion torque profile (bottom). Markers represent measurement points taken between half-turns of the screw. Insertion depth is the distance between the proximal tip of the screw and the surface of the bone (foam). Vertical hashed lines represent the screw position when the proximal tip is flush (0 mm) and buried (-2 mm) below the cortex.

after screw reinsertion,¹⁴ compression along the length of the screw,²¹ effect of central versus eccentric screw placement,^{26–28} pull-apart force,^{17,20,29} and failure under cyclical loading.^{9,10,29} The most widely studied parameter, however, is interfragmentary compression.^{11,12,17–19,22} Overall there is variability in absolute results between studies whereas the relative comparison between screws consistently shows that second-generation HCSs, such as the 4 screws in this study, outperform the original Herbert screw.

Why the emphasis on compression? Theoretically, the advantages are clear. Compression improves fracture stability and limits strain and shear along the fracture site, thereby facilitating primary bone healing.³⁰ Although many studies highlight the need to maximize compression, the absolute value needed for sufficient scaphoid fracture healing is unknown. Clinically, the impact of compression is even less certain. A retrospective study by Gregory and colleagues³¹ demonstrated no significant difference in union rate or time to union

would be clinically significant because the SD was only 2% to 16% of the mean.

The conically shaped, fully threaded design of the Acutrak perpetually generates compression as seen by a positive slope in the compression profile throughout most of insertion. Both the standard and the mini versions demonstrated a loss of compression as the trailing end of the screw leaves the cortex (1 mm dense foam layer); however, the compression is quickly regained as the threads tap into the deeper (cancellous) foam. The peak compression in these screws occurs at approximately –3 mm below the cortex, which is very close to the recommended and clinically desired safe insertion depth. Loss of compression at deeper insertion ensues as the leading threads begin to strip; however, this occurs beyond a clinically targeted screw depth. Insertion torque increased continuously with screw insertion, and the values for the Acutrak Standard were similar to those previously reported by Pensy et al.³³ The torque was approximately 50% higher for the Acutrak Standard screw than for the Mini, which is commensurate to the larger diameter and increased surface area with bone. The risk of rotating the proximal fragment and losing the reduction is greater when high insertion torque is required to advance the screw. Intuitively, it would appear that insertion torque directly correlates with compression force owing to the increased friction between bone and implant. Although both parameters increased together, the correlation between them was poor (Fig. 4). Insertion torque rose continuously with screw insertion, even when compression was lost.

The Synthes and Herbert-Whipple screws have a shanked design and generated their peak compression before the implants were fully buried in foam. Furthermore, some of the precompression applied to the Synthes screw was lost during insertion despite the differential thread pitch between ends, which is designed to augment compression throughout insertion. Nonetheless, both shanked screws demonstrated relatively stable insertion profiles, offering consistent compression over a wide range of insertion depths. The effect of traversing the denser foam (cortex) was less evident in these profiles. Similar to the Acutrak screws, the torque correlated poorly to compression and continued to increase even when compression was lost.

Limitations of this study include *ex vivo* evaluation, analysis limited to compression and insertion torque, and fracture simulation using a perfectly linear and perpendicular plane to the screw. These limitations

were needed to enable repeatable and reliable testing of the implants and are unlikely to affect the external validity of our findings.

Based on the insertion profiles generated in this study, several important findings were made. First, conically shaped HCSs generated their peak compression when they were fully buried in the foam whereas the shanked HCSs reached peak compression before they were fully inserted. This finding suggests that the Acutrak screws should be inserted at least 2 mm below the cortex and the Synthes and Herbert-Whipple would provide more optimal compression when the trailing end remains roughly flush with the cortex. Second, insertion torque was shown to correlate poorly with compression, peaking far after the point of maximum compression. Unlike standard, uniformly threaded screws, 1 end of the compression screw may be loose while the other is firmly engaged in bone, thereby generating high insertion torque with little compression. Surgeons should, therefore, avoid using tactile judgment of torque as a proxy for compression. Third, all 4 screws tested generated a sizable amount of compression (> 60 N or 6 kg) over a wide range of insertion depths. The actual compression at an insertion depth of 2 mm below the cortex was not significantly different between HCSs. Given that we do not know how much compression is required for bone healing and that all 4 screws provided comparable amounts of compression, implant selection should consider practical factors such as the ability to achieve adequate reduction, good implant placement, and familiarity with the implant specific instrumentation rather than compression alone.

REFERENCES

1. Hove LM. Epidemiology of scaphoid fractures in Bergen, Norway. *Scand J Plast Reconstr Surg Hand Surg.* 1999;33(4):423–426.
2. Duckworth AD, Jenkins PJ, Aitken SA, Clement ND, Court-Brown CM, McQueen MM. Scaphoid fracture epidemiology. *J Trauma.* Epub ahead of print 2011 Oct 13.
3. Van Tassel DC, Owens BD, Wolf JM. Incidence estimates and demographics of scaphoid fracture in the U.S. population. *J Hand Surg Am.* 2010;35(8):1242–1245.
4. Haisman JM, Rohde RS, Weiland AJ, American Academy of Orthopaedic Surgeons. Acute fractures of the scaphoid. *J Bone Joint Surg Am.* 2006;88(12):2750–2758.
5. Steinmann SP, Adams JE. Scaphoid fractures and nonunions: diagnosis and treatment. *J Orthop Sci.* 2006;11(4):424–431.
6. Herbert TJ, Fisher WE, Leicester AW. The Herbert bone screw: a ten year perspective. *J Hand Surg Br.* 1992;17(4):415–419.
7. Kawamura K, Chung KC. Treatment of scaphoid fractures and nonunions. *J Hand Surg Am.* J2008;33(6):988–997.
8. Fowler JR, Ilyas AM. Headless compression screw fixation of scaphoid fractures. *Hand Clin.* 2010;26(3):351–361, vi.
9. Toby EB, Butler TE, McCormack TJ, Jayaraman G. A comparison of fixation screws for the scaphoid during application of cyclical bending loads. *J Bone Joint Surg Am.* 1997;79(8):1190–1197.

10. Dodds SD, Panjabi MM, Slade JF III. Screw fixation of scaphoid fractures: a biomechanical assessment of screw length and screw augmentation. *J Hand Surg Am.* 2006;31(3):405–413.
11. Beadel GP, Ferreira L, Johnson JA, King GJ. Interfragmentary compression across a simulated scaphoid fracture—analysis of 3 screws. *J Hand Surg Am.* 2004;29(2):273–278.
12. Grewal R, Assini J, Sauder D, Ferreira L, Johnson J, Faber K. A comparison of two headless compression screws for operative treatment of scaphoid fractures. *J Orthop Surg Res.* 2011;6:27.
13. Gruszka DS, Burkhart KJ, Nowak TE, Achenbach T, Rommens PM, Muller LP. The durability of the intrascaphoid compression of headless compression screws: in vitro study. *J Hand Surg Am.* 2012;37(6):1142–1150.
14. Gardner AW, Yew YT, Neo PY, Lau CC, Tay SC. Interfragmentary compression profile of 4 headless bone screws: an analysis of the compression lost on reinsertion. *J Hand Surg Am.* 2012;37(9):1845–1851.
15. Faran KJ, Ichioka N, Trzeciak MA, Han S, Medige J, Moy OJ. Effect of bone quality on the forces generated by compression screws. *J Biomech.* 1999;32(8):861–864.
16. Brown GA, McCarthy T, Bourgeault CA, Callahan DJ. Mechanical performance of standard and cannulated 4.0-mm cancellous bone screws. *J Orthop Res.* 2000;18(2):307–312.
17. Baran O, Sagol E, Oxaz H, Sarikanat M, Havitcioglu H. A biomechanical study on preloaded compression eVect on headless screws. *Arch Orthop Trauma Surg.* 2009;129(12):1601–1605.
18. Adla DN, Kitsis C, Miles AW. Compression forces generated by Mini bone screws—a comparative study done on bone model. *Injury.* 2005;36(1):65–70.
19. Hausmann JT, Mayr W, Unger E, Benesch T, Vecsei V, Gabler C. Interfragmentary compression forces of scaphoid screws in a saw-bone cylinder model. *Injury.* 2007;38(7):763–768.
20. Crawford LA, Powell ES, Trail IA. The fixation strength of scaphoid bone screws: an in vitro investigation using polyurethane foam. *J Hand Surg Am.* 2012;37(2):255–260.
21. Sugathan HK, Kilpatrick M, Joyce TJ, Harrison JW. A biomechanical study on variation of compressive force along the Acutrak 2 screw. *Injury.* 2012;43(2):205–208.
22. Bailey CA, Kuiper JH, Kelly CP. Biomechanical evaluation of a new composite bioresorbable screw. *J Hand Surg Br.* 2006;31(2):208–212.
23. Laboratories PR. Available at <https://http://www.sawbones.com/products/bio/testblocks/solidfoam.aspx>. Accessed Nov 2012.
24. Qu G, von Schroeder HP. Trabecular microstructure at the human scaphoid nonunion. *J Hand Surg Am.* 2008;33(5):650–655.
25. Lee SB, Kim HJ, Chun JM, et al. Osseous microarchitecture of the scaphoid: cadaveric study of regional variations and clinical implications. *Clin Anat.* 2012;25(2):203–211.
26. McCallister WV, Knight J, Kaliappan R, Trumble TE. Central placement of the screw in simulated fractures of the scaphoid waist: a biomechanical study. *J Bone Joint Surg Am.* 2003;85(1):72–77.
27. Luria S, Hoch S, Liebergall M, Mosheiff R, Peleg E. Optimal fixation of acute scaphoid fractures: finite element analysis. *J Hand Surg Am.* 2010;35(8):1246–1250.
28. Hart A, Mansuri A, Harvey EJ, Martineau PA. Central versus eccentric internal fixation of acute scaphoid fractures. *J Hand Surg Am.* 2013;38(1):66–71.
29. Wheeler DL, McLoughlin SW. Biomechanical assessment of compression screws. *Clin Orthop Relat Res.* 1998;350:237–245.
30. Augat P, Burger J, Schorlemmer S, Henke T, Peraus M, Claes L. Shear movement at the fracture site delays healing in a diaphyseal fracture model. *J Orthop Res.* 2003;21(6):1011–1017.
31. Gregory JJ, Mohil RS, Ng AB, Warner JG, Hodgson SP. Comparison of Herbert and Acutrak screws in the treatment of scaphoid non-union and delayed union. *Acta Orthop Belg.* 2008;74(6):761–765.
32. Oduwole KO, Cichy B, Dillon JP, Wilson J, O’Beirne J. Acutrak versus Herbert screw fixation for scaphoid non-union and delayed union. *J Orthop Surg (Hong Kong).* 2012;20(1):61–65.
33. Pensy RA, Richards AM, Belkoff SM, Mentzer K, Andrew Eglseider W. Biomechanical comparison of two headless compression screws for scaphoid fixation. *J Surg Orthop Adv Winter.* 2009;18(4):182–188.